



Transport Delay and First Order Inertia Time Signal Prediction Dedicated to Teleoperation

Mateusz Saków^(✉) and Karol Miądlicki

Faculty of Mechanical Engineering and Mechatronics, West Pomeranian
University of Technology, 19 Piastów Avenue, 70-310 Szczecin, Poland
{mateusz.sakow, karol.miadlicjk}@zut.edu.pl

Abstract. In the paper a sensor-less control scheme for a bilateral teleoperation system with a force-feedback based on a prediction of an input of a non-linear inverse model by prediction blocks is presented. The prediction method was designed to minimize the effect of the transport delay and the phase shift of sensors, actuators and mechanical objects. The solution is an alternative to complex non-linear models like artificial neural networks, which requires complex stability analysis and control systems with high computing power. Also, in this paper we had compared a transport delay and first order inertia continues approach. The effectiveness of both approaches has been verified on the hydraulic manipulator test stand.

Keywords: Force-feedback · Bilateral teleoperation · Model-free prediction

1 Introduction

Nearly for an age, a research is being carried out to obtain remotely control human operation systems [4, 29]. The purpose of these efforts is dedicated to development of a device that will separate an operator of such a system from a hazardous environment [39]. It is possible to mention many exemplars as: (1) nuclear power plants reactor operations; (2) any work carried outside spacecrafts; (3) under water and deep sea manipulation where these kind of devices can find their usefulness [7]. However, from early 60's of the previous century, research is being carried out to obtain remote manipulation which is supported by haptic interfaces [7, 8, 44].

The problem of stability and a counteract of the effect of the delay in the communication channel affecting the system operation, are addressed by many scientific papers [7, 16, 17, 26]. First methods maintaining the stability were the move-and-wait strategy and the deliberate slowdown of operator motion when approaching the environmental object was presented by Ferrell [7]. However, control strategies presented in [7], did not gave such a results of task time completion, as the adaptive control which was introduced in [26]. Later, sensor based control schemes presented in [7] was redesigned and equipped with a shared compliant control method by Kim [17]. However, none of these control schemes could guaranteed the stability of the entire system, when large delays were expected in the communication channel. Only after the modification of communication channel based on a wave variables allowed bilateral teleoperation systems to maintain stability regardless to the delay in the communication

channel [37]. During further research, wave variables were extended with the passivity formalism [1], and optimization methods for degradation in performance [6]. However, a significant improvement of force projection in the force-feedback communication channel was reached by the four-channel architecture [11, 18]. The four-channel architecture is characterized by a two-way force and position transfer between sub-systems Master and Slave.

XXI century is a time of control schemes implementation, which are based on: sliding mode controllers [13, 24, 25]; fuzzy logic controllers [5]; force-feedback communication channel frequency separation techniques [2, 28]; special methods for discretization of a sensor resolution [12]; artificial neural networks [42]; and adaptive controllers dedicated to variable and asymmetric time delays, which were extended by using of adaptive filtering methods [46, 47]. There are even methods, which are dedicated to a model-free prediction in the communication channel [10, 30]. However, it is important to pay attention that bilateral teleoperation systems feature three types of feedback with the operator: vision-feedback [9, 38]; force-feedback [7] and combination of vision-feedback and force-feedback [3, 11, 16, 17, 42, 43, 48]. Furthermore, there are methods, which are dedicated to real-time monitoring of the remote environment [20, 22, 23, 27]. Remotely controlled devices could be controlled by operator's motion scanners [7–9, 16, 17, 32, 38], which in a special case are exoskeletons for an upper limb [32], by gesture control techniques [21, 27] or by voice control methods [40, 41]. However, the use of a voice control or a gesture control allows to use only the vision-feedback between the operator and remotely controlled device. Also an important classification of bilateral teleoperation systems with force-feedback are systems which are using force sensor [2, 7, 17, 28] and devices without force sensors, also known as a sensor-less or self-sensing techniques in the telemanipulation field [15, 29, 32, 42, 45]. The sensor-less teleoperation systems group usually is based on impedance control [13] and the inverse modeling techniques [42], to obtain correct value of force in the force-feedback communication channel [31–36, 45]. Inverse models are represented frequently by artificial neural networks [42], nonlinear autoregressive model with exogenous inputs (NARX) [32] and by micromanipulators which are using reversal processes that occur in piezo-crystals [29].

The paper addresses the transport delay problem in a sensor-less control scheme based on a dynamic inverse modeling procedure, which allows the system to estimate environmental force affecting the Slave manipulator body. The dynamic inverse model used in the control unit was extended with proposed prediction blocks. The single prediction block has been a phase shifter with specific characteristics. The characteristics of the prediction block is a strongly linear phase diagram in a useful frequency spectrum, which allows the system to predict the manipulator motion with a close to constant time shift. The proposed nonlinear inverse dynamic model structure, which a nonlinearity has included the modified friction model based on the Stribeck friction interpretation was validated at a 1-DoF (1 Degree of Freedom) hydraulic manipulator test stand. During the experiment and simulations, it was confirmed the effectiveness of a prediction of input of the nonlinear inverse model in both approaches, by reducing the time phase shift error between measured and simulated control signals.

2 Inverse Model Based Bilateral Teleoperation with Prediction

A Schematic diagram of the entire Master-Slave system with force-feedback is presented in the Fig. 1.

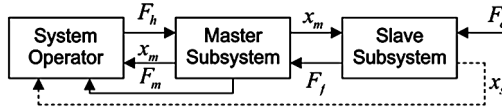


Fig. 1. The Master-Slave system with force-feedback.

The system structure contains 3 specific objects: the operator block which controls the position of the Master subsystem (motion scanner) by affecting it with a human force F_h . The Master subsystem transfers its position x_m to the Slave subsystem. The control unit of the Slave subsystem seeks to obtain the position of the Master subsystem by the Slave subsystem $x_s \cong x_m$. In the force-feedback channel F_f environmental force influence F_e is being transfer back to the Master subsystem. The second task of the motion scanner, is to deliver the force from the force-feedback channel back to the operator $F_m \cong F_e$. However, the value of the force F_m strongly depends on the inverse model accuracy [32]. In practice, obtaining an ideal inverse model of any subsystem is impossible, but there are methods, which allows us to get a little bit closer to the description of a reality. One of these methods is presented in the Sect. 2.

After introduction of the prediction technique used in the inverse modeling method [34], in the paper a prediction block frequency analysis were introduced presented. The prediction block and its structure was developed during the analysis of the Smith predictive control schemes [14] – Fig. 2.

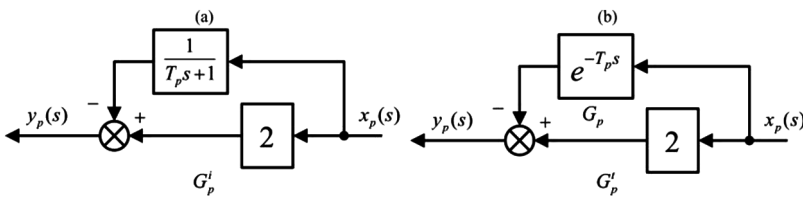


Fig. 2. (a) First order inertia based prediction block, (b) Transport delay based prediction block.

In the case of the first order inertia, the transmittance $G_p^i(s)$ characterizing the automation structure in the Fig. 2a, is described by a ratio of an output signal $y_p(s)$ to an input signal $x_p(s)$, and is given by Eq. (1):

$$G_p^i(s) = y_p(s)/x_p(s) = (2T_p s + 1)/(T_p s + 1), \tag{1}$$

where s is the Laplace operator. Otherwise, the transmittance $G_p^t(s)$ characterizing the automation structure in the Fig. 2b, is described by a ratio of an output signal $y_p(s)$ to an input signal $x_p(s)$ also, but is given by Eq. (2):

$$G_p^t(s) = y_p(s)/x_p(s) = 2 - e^{-T_p s}, \tag{2}$$

where in both cases the T_p is a value of the constant time shift, thus the prediction.

Examining the transmittance (1) and (2) in the frequency domain it has to be paid attention to the amplitude (Fig. 3a) and phase diagram (Fig. 3b) of the prediction blocks presented in the Fig. 3.

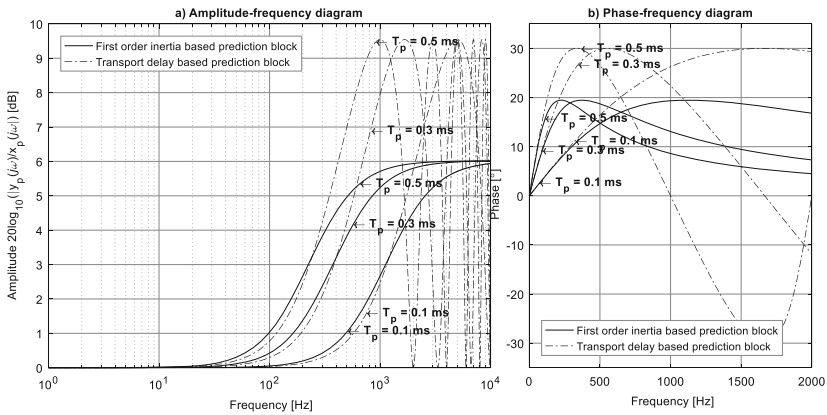


Fig. 3. (a) Amplitude-frequency diagram, (b) Phase-frequency diagram of the prediction blocks.

The prediction block which depends on the T_p coefficient is able to linearly shift a phase of an input signal, resulting in a constant time shift in a useful frequency spectrum – Fig. 3b. The transport delay approach remains closer to a linear characteristic for a wider frequency spectrum, with a respect to the first order inertia based prediction block. The prediction block like any phase shifter is a cause of a gain of the input signal amplitude, but in the useful frequency range the gain is closer to a unity – Fig. 3a. The prediction block, which is based on a transport delay is closer to a unit for wider frequency spectrum, and it creates a possibility to not increase the controller’s quantum noise amplitude. At the cost of this feature is a higher gain for a transition frequency spectrum. The useful frequency spectrum is understood to be the achievable for a human motion. Scientific literature gives a limit of a 6 Hz [19].

Both frequency diagrams in Fig. 3 are the proof of predictive capabilities of the prediction block. The prediction block in a time domain is a “signal predictor” of the input signal $x_p(t)$, where predicted time depends only on the T_p constant. However, is important to note, that the first order inertia based prediction block is sensitive to a noise, while the transport prediction block is more sensitive to a transition frequency spectrum, and both are sensitive to changes of a signal derivative sign $x_p(t)$.

3 Simulations of Prediction Models

In papers [32, 42], estimated value by the inverse model was a pneumatic air pressure in a chamber of an actuator, which has caused a motion of a piston. However, a measurement of the pneumatic air pressure is affected by a significant delay [34]. In the paper, it was decided to estimate an environmental force based on the control signal, which is well-known. The inverse dynamic model in this case was used for estimation of a control signal, which was required for free-motion of a Slave manipulator in a single joint. The next step was a signals subtraction. The estimated control signal was subtracted from the known control signal applied to the object. After that, the estimated control signal in the proposed control scheme was calculated by the inverse model G^{-1} , which input was the position x_s in a Slave manipulator joint – Fig. 4.

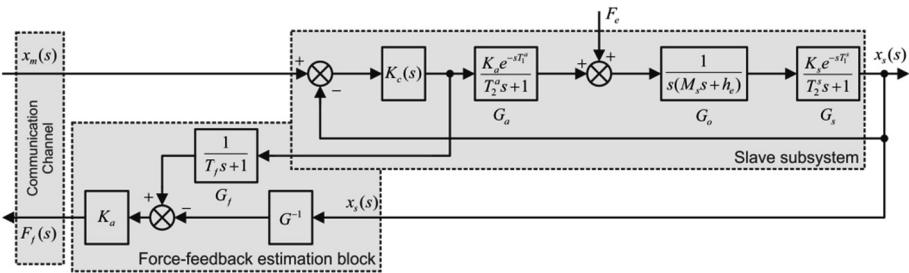


Fig. 4. Control unit scheme of the Slave subsystem with force-feedback estimation block.

The control unit scheme describes the Slave subsystem with a dual channel based communication architecture. The Slave consists of a controller $K_c(s)$, an actuator $G_a(s)$ (with a gain K_a , a transport delay T_1^a and a first order inertia T_2^a parameters), an object $G_o(s)$ (with a mass M_s and a damping h_e parameters) and a sensor $G_s(s)$ (with a gain K_s , a transport delay T_1^s and a first order inertia T_2^s parameters) transfer functions. The estimation block consists the inverse model G^{-1} , a low-pass filter $G_f(s)$ with a parameter T_f and a gain K_a , same as in the actuator’s transfer function. In the case of a known inverse model, which describes Slave subsystem, it is obvious that it consists of an exponential function with a positive parameter: $e^{s(T_1^a + T_1^s)}$. The difference between the object control signal and the estimated control signal in free-motion increased by the K_a gain, and described by the force $F_f(s)$ in the force-feedback channel is equal to the environmental force $F_f(s) = F_e(s)$.

To minimize the effect of a transport delay, in the force-feedback communication channel, two prediction blocks have been implemented into the structure of the inverse model, and replaced the exponential function with a positive parameter. The proposed inverse model is described by the Eq. (3) for first inertia model and the Eq. (4) for transport delay approach:

$$G^{-1} = \frac{s(2T_p s + 1)(h_e + M_s s)(T_2^a s + 1)(T_2^s s + 1)}{K_a K_s (T_p s + 1)(T_f s + 1)}, \quad (3)$$

$$G^{-1} = (2 - e^{-T_p s}) \frac{s(h_e + M_s s)(T_2^a s + 1)(T_2^s s + 1)}{K_a K_s (T_f s + 1)}. \quad (4)$$

Subsystem in the Fig. 4 was analyzed during multiple simulations. The comparison of the linear models given by the Eqs. (3) and (4), and the standard 5th order transfer function with an equal degree of the polynomial in the numerator and the denominator. The simulation was carried for the data: $K_a = 1$; $K_s = 1$; $T_1^a = 0.002$; $T_2^a = 0.002$; $M_s = 10$; $h_e = 1$; $T_1^s = 0.002$; $T_2^s = 0.002$; $F_e = 0$; $T_f = 0,0005$ and $x_m(t)$ was a harmonic signal with variable frequency in the range of a 0.1 Hz to 10 Hz. The results are presented in the Fig. 5.

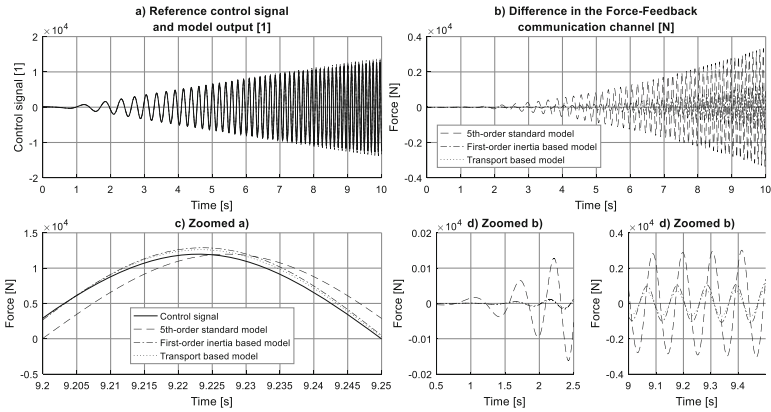


Fig. 5. Simulation results of the system without and with a both prediction approaches.

Simulation results confirms that the inverse model which structure included prediction blocks is able to predict the control signal with a higher accuracy than the same order model obtained by a standard MATLAB identification techniques. However, the transport delay based inverse model is characterized by a 25% lower error of control signal estimation for frequencies closer to a 10 Hz, according to the first-order inertia based predictive model. The difference is unnoticeable for frequencies tending to 0 Hz. In simulations the noise effect was not taken into account.

4 Experiment

The method based on a prediction, was validated at a 1-DoF hydraulic linear manipulator [34–36]. The position of the manipulator was measured by two inductive sensors, which average signal was used in the control unit. The measured and estimated

control signal by the inverse model, was a valve current. The inverse model has a structure presented by the Eqs. (3) and (4), but included a nonlinear component describing the damping force $F_{h_{e,s}}$ given by the Eq. (5):

$$F_{h_{e,s}}(t) = \left(\frac{1}{1 + e^{(-v_s(t))}} - \frac{v_s(t) + 5}{10} + 0.00045v_s(t)|v_s(t)| \right) h_e. \quad (5)$$

where $v_s(t) = dx_s(t)/dt$.

For two prediction blocks, the T_p coefficient was identified at 0.0018 during the manipulator movement during iterative procedure. The implementation of prediction blocks allowed to minimize the current mean absolute error from 0.55 mA to 0.39 mA for the first order inertia based model, and to 0.38 mA for transport delay based model, when a chirp signal response was used as a comparison of an input signal. This is a significant difference, which allowed to reduce the estimation error about +30% for both approaches. The force in the force-feedback communication channel during rigid contact task is presented in the Fig. 6.

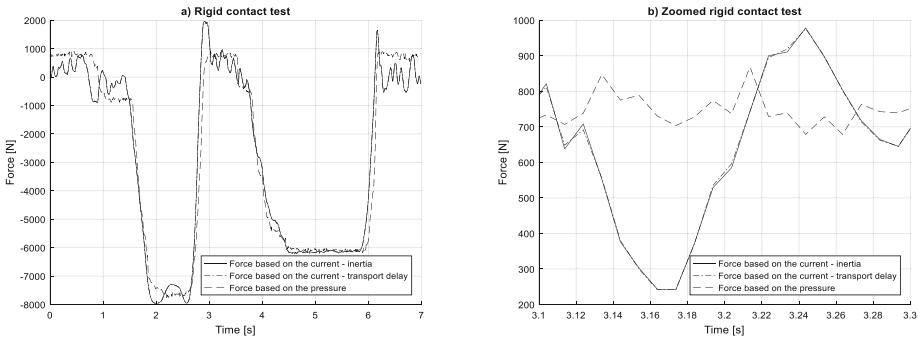


Fig. 6. Force-feedback communication channel during rigid contact test.

During the multiply experiments, there we had carried out a standard identification of a 4th order inverse model. In most of the experiments this model turned out to be unstable. For this reason, it was only used for offline comparison to the experimental data, while the identification included the Tikonov regularization. Then, before the operator took part in the rigid contact test, the operator was obliged to move the manipulator body until the piston will reach its maxim position and will touch made of steel movement boundaries. In both approaches, the method allowed the system to predict the environmental force up to 200 ms faster than it could be sensed by the pressure sensor during free motion (Fig. 6, time period from 0.5 s to 1 s). In the force-feedback channel force was reduced a hundred times because of the hydraulic manipulator was able to generate a force of 20 kN.

5 Conclusion

The paper presents a novel approach to a control design in bilateral and sensor-less teleoperation systems based on the prediction of an input and an output of an inverse model. The technique was based on simple prediction blocks, which each prediction block was a phase shifter having specific properties. The paper presented prediction blocks analysis in frequency domain. The inverse model was implemented in the control unit of the test stand and series of tests were carried out. Experimental results confirmed that the system equipped with the proposed method based on two approaches is able to predict the environmental force impact with relatively high accuracy.

Acknowledgments. The work was carried out as part of the PBS3/A6/28/2015 project, “The use of augmented reality, interactive voice systems and operator interface to control a crane”, financed by NCBiR.

References

1. Arcara, P., Melchiorri, C., Stramigioli, S.: Intrinsically passive control in bilateral teleoperation mimo systems. In: 2001 European Control Conference (ECC), pp. 1180–1185 (2001)
2. Atashzar, S.F., Polushin, I.G., Patel, R.V.: Projection-based force reflection algorithms for teleoperated rehabilitation therapy. In: 2013 IEEE/RSJ International Conference on Intelligent Robots and Systems, pp. 477–482 (2013)
3. Ben-Dov, D., Salcudean, S.E.: A force-controlled pneumatic actuator for use in teleoperation masters. In: Proceedings of the 1993 IEEE International Conference on Robotics and Automation, vol. 933, pp. 938–943 (1993)
4. C GR: Remote-control manipulator. Google Patents (1953)
5. Chang, M.-K.: An adaptive self-organizing fuzzy sliding mode controller for a 2-DoF rehabilitation robot actuated by pneumatic muscle actuators. *Control Eng. Pract.* **18**, 13–22 (2010)
6. Ferraguti, F., Fantuzzi, C., Secchi, C.: Optimizing the use of power in wave based bilateral teleoperation. In: 2016 IEEE/RSJ International Conference on Intelligent Robots and Systems (IROS), pp. 1469–1474. IEEE (2016)
7. Ferrell, W.R.: Delayed force feedback. *Hum. Factors J. Hum. Factors Ergon. Soc.* **8**, 449–455 (1966)
8. Ferrell, W.R.: Remote manipulation with transmission delay. *IEEE Trans. Hum. Factors Electron. HFE* **6**, 24–32 (1965)
9. Ferrell, W.R., Sheridan, T.B.: Supervisory control of remote manipulation. *IEEE Spectr.* **4**, 81–88 (1967)
10. Ge, X., Zheng, Y., Brudnak, M.J., et al.: Analysis of a model-free predictor for delay compensation in networked systems. In: *Time Delay Systems*, pp. 201–215. Springer, Cham (2017)
11. Hastrudi-Zaad, K., Salcudean, S.E.: On the use of local force feedback for transparent teleoperation. In: Proceedings of the 1999 IEEE International Conference on Robotics and Automation, vol. 1863, pp. 1863–1869 (1999)
12. Hulin, T., Albu-Schäffer, A., Hirzinger, G.: Passivity and stability boundaries for haptic systems with time Delay. *IEEE Trans. Control Syst. Technol.* **22**, 1297–1309 (2014)

13. Hyun Chul, C., Jong Hyeon, P., Kyunghwan, K., et al.: Sliding-mode-based impedance controller for bilateral teleoperation under varying time-delay. In: Proceedings of the 2001 IEEE International Conference on Robotics and Automation, ICRA, vol. 1021, pp. 1025–1030 (2001)
14. Kaya, I.: Obtaining controller parameters for a new PI-PD Smith predictor using autotuning. *J. Process Control* **13**, 465–472 (2003)
15. Khadraoui, S., Rakotondrabe, M., Lutz, P.: Interval modeling and robust control of piezoelectric microactuators. *IEEE Trans. Control Syst. Technol.* **20**, 486–494 (2012)
16. Kim, W.S.: Developments of new force reflecting control schemes and an application to a teleoperation training simulator. In: Proceedings of the 1992 IEEE International Conference on Robotics and Automation, vol. 1412, pp. 1412–1419 (1992)
17. Kim, W.S., Hannaford, B., Fejczy, A.K.: Force-reflection and shared compliant control in operating telemanipulators with time delay. *IEEE Trans. Robot. Autom.* **8**, 176–185 (1992)
18. Lawrence, D.A.: Stability and transparency in bilateral teleoperation. *IEEE Trans. Robot. Autom.* **9**, 624–637 (1993)
19. Lichardopol, S., Wouw, N.V.D., Nijmeijer, H.: Control scheme for human-robot co-manipulation of uncertain, time-varying loads. In: 2009 American Control Conference, pp. 1485–1490 (2009)
20. Miądlicki, K., Pajor, M., Sakow, M.: Loader crane working area monitoring system based on LIDAR scanner. In: *Advances in Manufacturing*, p. 465 (2017)
21. Miądlicki, K., Pajor, M.: Real-time gesture control of a CNC machine tool with the use Microsoft Kinect sensor. *Int. J. Sci. Eng. Res.* **6**, 538–543 (2015)
22. Miądlicki, K., Pajor, M., Saków, M.: Ground plane estimation from sparse LIDAR data for loader crane sensor fusion system. In: 2017 22nd International Conference on Methods and Models in Automation and Robotics (MMAR), pp. 717–722. IEEE (2017)
23. Miądlicki, K., Pajor, M., Saków, M.: Real-time ground filtration method for a loader crane environment monitoring system using sparse LIDAR data. In: 2017 IEEE International Conference on INnovations in Intelligent SysTems and Applications (INISTA), pp. 207–212. IEEE (2017)
24. Moreau, R., Pham, M.T., Tavakoli, M., et al.: Sliding-mode bilateral teleoperation control design for master–slave pneumatic servo systems. *Control Eng. Pract.* **20**, 584–597 (2012)
25. Nguyen, T., Leavitt, J., Jabbari, F., et al.: Accurate sliding-mode control of pneumatic systems using low-cost solenoid valves. *IEEE/ASME Trans. Mechatron.* **12**, 216–219 (2007)
26. Niemeyer, G., Slotine, J.J.E.: Stable adaptive teleoperation. *IEEE J. Ocean. Eng.* **16**, 152–162 (1991)
27. Pajor, M., Miądlicki, K., Saków, M.: Kinect sensor implementation in fanuc robot manipulation. *Arch. Mech. Technol. Autom.* **34**, 35–44 (2014)
28. Polushin, I.G., Takhmar, A., Patel, R.V.: Projection-based force-reflection algorithms with frequency separation for bilateral teleoperation. *IEEE/ASME Trans. Mechatron.* **20**, 143–154 (2015)
29. Rakotondrabe, M., Ivan, I.A., Khadraoui, S., et al.: Simultaneous displacement/force self-sensing in piezoelectric actuators and applications to robust control. *IEEE/ASME Trans. Mechatron.* **20**, 519–531 (2015)
30. Sakow, M., Parus, A., Pajor, M., et al.: Unilateral hydraulic telemanipulation system for operation in machining work area. In: *Advances in Manufacturing*, p. 415 (2017)
31. Saków, M., Miądlicki, K., Parus, A.: Self-sensing teleoperation system based on 1-dof pneumatic manipulator. *J. Autom. Mob. Robot. Intell. Syst.* **11**, 64–76 (2017)
32. Saków, M., Pajor, M., Parus, A.: Estymacja siły oddziaływania środowiska na układ zdalnie sterowany ze sprzężeniem siłowym zwrotnym o kinematyce kończyny górnej. *Modelowanie Inz.* **58**, 113–122 (2016)

33. Saków, M., Pajor, M., Parus, A.: Układ sterowania samowyznaczający siły oddziaływania środowiska na manipulator wykonawczy w czasie pracy systemu telemanipulacyjnego. *Projektowanie Mechatroniczne - Zagadnienia Wybrane*, pp. 139–150. Katedra Robotyki i Mechatroniki, Akademia Górniczo-Hutnicza w Krakowie (2016)
34. Saków, M., Parus, A.: Sensorless control scheme for teleoperation with force-feedback, based on a hydraulic servo-mechanism, theory and experiment. *Measur. Autom. Monit.* **62**, 417–425 (2016)
35. Saków, M., Parus, A., Miądlicki, K.: Predykcyjna metoda wyznaczania siły w siłowym sprzężeniu zwrotnym w systemie zdalnie sterowanym. *Modelowanie Inż.* **31**, 88–97 (2017). (in Polish)
36. Saków, M., Parus, A., Pajor, M., et al.: Nonlinear inverse modeling with signal prediction in bilateral teleoperation with force-feedback. In: *2017 22nd International Conference on Methods and Models in Automation and Robotics (MMAR)*, pp. 141–146. IEEE (2017)
37. Sheridan, T.B.: Space teleoperation through time delay: review and prognosis. *IEEE Trans. Robot. Autom.* **9**, 592–606 (1993)
38. Sheridan, T.B., Ferrell, W.R.: Human control of remote computer-manipulators. In: *Proceedings of the 1st International Joint Conference on Artificial Intelligence*, Washington, DC, pp. 483–494. Morgan Kaufmann Publishers Inc. (1969)
39. Sheridan, T.B., Verplank, W.L.: Human and computer control of undersea teleoperators. *Massachusetts Inst. of Tech. Cambridge Man-Machine Systems Lab.* (1978)
40. Stuart, K.D., Majewski, M.: Intelligent opinion mining and sentiment analysis using artificial neural networks. In: *International Conference on Neural Information Processing*, pp. 103–110. Springer, Cham (2015)
41. Stuart, K.D., Majewski, M., Trelis, A.B.: Intelligent semantic-based system for corpus analysis through hybrid probabilistic neural networks. In: *International Symposium on Neural Networks*, pp. 83–92. Springer, Heidelberg (2011)
42. Tadano, K., Kawashima, K.: Development of 4-DOFs forceps with force sensing using pneumatic servo system. In: *Proceedings 2006 IEEE International Conference on Robotics and Automation, ICRA 2006*, pp. 2250–2255 (2006)
43. Tavakoli, M., Patel, R.V., Moallem, M.: A force reflective master-slave system for minimally invasive surgery. In: *Proceedings of the 2003 IEEE/RSJ International Conference on Intelligent Robots and Systems (IROS 2003)*, vol. 3073, pp. 3077–3082 (2003)
44. Tomovic, R., Boni, G.: An adaptive artificial hand. *IRE Trans. Autom. Control* **7**, 3–10 (1962)
45. Wei Tech, A., Khosla, P.K., Riviere, C.N.: Feedforward controller with inverse rate-dependent model for piezoelectric actuators in trajectory-tracking applications. *IEEE/ASME Trans. Mechatron.* **12**, 134–142 (2007)
46. Zhai, D.H., Xia, Y.: Adaptive control for teleoperation system with varying time delays and input saturation constraints. *IEEE Trans. Ind. Electron.* **63**, 6921–6929 (2016)
47. Zhai, D.H., Xia, Y.: Adaptive control of semi-autonomous teleoperation system with asymmetric time-varying delays and input uncertainties. *IEEE Trans. Cybern.* **47**(11), 3621–3633 (2016)
48. Zhou, M., Ben-Tzvi, P.: RML glove – an exoskeleton glove mechanism with haptics feedback. *IEEE/ASME Trans. Mechatron.* **20**, 641–652 (2015)